



HAL
open science

The ectodomain of the viral receptor YueB forms a fiber that triggers ejection of bacteriophage SPP1 DNA.

Carlos São-José, Sophie Lhuillier, Rudi Lurz, Ronald Melki, Jean Lepault,
Mário Almeida Santos, Paulo Tavares

► To cite this version:

Carlos São-José, Sophie Lhuillier, Rudi Lurz, Ronald Melki, Jean Lepault, et al.. The ectodomain of the viral receptor YueB forms a fiber that triggers ejection of bacteriophage SPP1 DNA.. *Journal of Biological Chemistry*, 2006, 281 (17), pp.11464-70. 10.1074/jbc.M513625200 . hal-01183828

HAL Id: hal-01183828

<https://hal.science/hal-01183828>

Submitted on 30 May 2020

HAL is a multi-disciplinary open access archive for the deposit and dissemination of scientific research documents, whether they are published or not. The documents may come from teaching and research institutions in France or abroad, or from public or private research centers.

L'archive ouverte pluridisciplinaire **HAL**, est destinée au dépôt et à la diffusion de documents scientifiques de niveau recherche, publiés ou non, émanant des établissements d'enseignement et de recherche français ou étrangers, des laboratoires publics ou privés.

Copyright

The Ectodomain of the Viral Receptor YueB Forms a Fiber That Triggers Ejection of Bacteriophage SPP1 DNA*

Received for publication, December 21, 2005, and in revised form, February 14, 2006. Published, JBC Papers in Press, February 14, 2006, DOI 10.1074/jbc.M513625200

Carlos São-José^{‡1}, Sophie Lhuillier^{§2}, Rudi Lurz[¶], Ronald Melki^{||}, Jean Lepault[§], Mário Almeida Santos[‡], and Paulo Tavares^{§3}

From the [‡]Faculdade de Ciências de Lisboa, Instituto de Ciência Aplicada e Tecnologia e Departamento de Biologia Vegetal, 1749-016 Lisboa, Portugal, [§]Unité de Virologie Moléculaire et Structurale, Unité Mixte de Recherche CNRS 2472, Unité Mixte de Recherche Institut Nationale, de la Recherche Agronomique 1157 and Institut Fédératif de Recherche 115, Bâtiment 14B, Avenue de la Terrasse, 91198 Gif-sur-Yvette cedex, France, [¶]Max-Planck-Institut für Molekulare Genetik, Ihnestrasse 73, 14195 Berlin, Germany, and ^{||}Laboratoire d'Enzymologie et Biochimie Structurales CNRS, Bâtiment 34, Avenue de la Terrasse, 91198 Gif-sur-Yvette cedex, France

The irreversible binding of bacteriophages to their receptor(s) in the host cell surface triggers release of the naked genome from the virion followed by transit of viral DNA to the host cell cytoplasm. We have purified, for the first time, a receptor from a Gram-positive bacterium that is active to trigger viral DNA ejection *in vitro*. This extracellular region ("ectodomain") of the *Bacillus subtilis* protein YueB (YueB780) was a 7 S elongated dimer forming a 36.5-nm-long fiber. YueB780 bound to the tail tip of bacteriophage SPP1. Although a stable receptor-phage interaction occurred between 0 and 37 °C, complete blocking of phage DNA release or partial ejection events were observed at temperatures below 15 °C. We also showed that the receptor was exposed to the *B. subtilis* surface. YueB differed structurally from phage receptors from Gram-negative bacteria. Its properties revealed a fiber spanning the full length of the 30-nm-thick peptidoglycan layer. The fiber is predicted to be anchored in the cell membrane through transmembrane segments. These features, highly suitable for a virus receptor in Gram-positive bacteria, are very likely shared by a large number of phage receptors.

Virus interaction with one or several cellular receptors is an essential step for recognition of the host cell and for commitment of the virus to initiate infection. Animal, plant, fungi, Archaea, and bacterial cells have different surfaces that impose distinct barriers for virus entry. Strategies to overcome these barriers and the receptors targeted by viruses are expectedly different (1, 2). More than 95% of the known bacterial viruses (bacteriophages) use a tail structure to recognize the host cell surface and to deliver their double-stranded DNA genome to the bacterial cytoplasm. The DNA enters naked into the cell, with the empty phage particle remaining in the exterior of the bacterium (3). Phage adsorption to

bacteria involves the specific interaction between tail adhesins and surface-exposed receptors of the host cell envelope. Adsorption of a particular phage may involve more than one cellular receptor, and binding can occur in a reversible or irreversible manner (4).

Phage receptors are found in surface-exposed organelles, such as flagella or pili, in the outer membrane of Gram-negative bacteria and in the thick peptidoglycan cell wall of Gram-positive bacteria (1, 2). Porins, affinity transporters, and lipopolysaccharides are the most common outer membrane components that act as receptors for tailed phages infecting Gram-negative bacteria (2). Outer membrane proteins known to act as phage receptors have been purified and their structures determined (5–7). They all share a channel-forming, β -barrel region organized by a variable number of antiparallel β -strands and can function as monomeric (FhuA) or trimeric (OmpA, OmpC, LamB) proteins (5–7).

The structures of phage receptors in Gram-positive bacteria is unknown. It is thought that phages initially adsorb in a reversible way to a general component of the cell wall prior to irreversible binding to a specific receptor (8, 9). The proteins GamR (*Bacillus anthracis*) (10), Pip (*Lactococcus lactis*) (11), and its orthologue YueB (*Bacillus subtilis*) (12) were identified genetically as phage receptors. Here we have described the purification and biochemical characterization of the YueB ectodomain harboring the SPP1 receptor activity (YueB780). The dimeric receptor was a 36.5-nm fiber that bound strongly to the tail tip of the SPP1 non-contractile tail and triggered DNA ejection *in vitro*. This was the first active virus receptor purified from Gram-positive bacteria. Its properties were significantly different from the known phage receptors of Gram-negative bacteria.

EXPERIMENTAL PROCEDURES

Bacterial Strains, Phages, and Plasmids—*B. subtilis* YB886 (13) was used for infection with bacteriophage SPP1 wild type as described previously (14). *B. subtilis* CJS1 and CJS3 (12) were used for the immunolabeling experiments of YueB at the bacterial surface. *E. coli* CG61 is a derivative of strain BL21 (Stratagene) harboring plasmid pGP1–2, which expresses T7 RNA polymerase gene 1 upon thermoinduction (15). *E. coli* CG61 cells transformed with plasmids pIVEX2.3d (Roche Applied Science) or pCSJ65 were selected in medium supplemented with ampicillin (100 μ g/ml) and kanamycin (40 μ g/ml). Construct pCSJ65 (12) is a pIVEX2.3d derivative carrying a truncated version of the receptor gene *yueB*. It codes for a polypeptide composed of YueB residues from positions 30–797 C-terminally fused to a hexahistidine-containing tag (YueB780) (Fig. 1). All strains were grown in LB at 37 °C, with the exception of *E. coli* CG61, which was grown at 28 °C.

* This work was supported by Grant POCTI/BIA-MIC/57088/2004 from Fundação para a Ciência e Tecnologia (FCT, Portugal) (to C. S.-J.), by an Action Thématique et Incitative sur Programme from CNRS (France) (to P. T.), and by the program "Dynamique et Réactivité des Assemblages Biologiques." The costs of publication of this article were defrayed in part by the payment of page charges. This article must therefore be hereby marked "advertisement" in accordance with 18 U.S.C. Section 1734 solely to indicate this fact.

¹ Supported by the post-doctoral fellowship BPD/9429/2002 from FCT (Portugal). To whom correspondence may be addressed: Instituto de Ciência Aplicada e Tecnologia e Departamento de Biologia Vegetal, Faculdade de Ciências de Lisboa, Ed. ICAT, 1749-016 Lisboa, Portugal. Tel.: 351-217500000 (ext. 20151); Fax: 351-217500048; E-mail: cjsjose@fc.ul.pt.

² Financed by a doctoral fellowship from the Ministère de l'Éducation Nationale de la Recherche et de la Technologie (France).

³ To whom correspondence may be addressed: Unité de Virologie Moléculaire et Structurale, Unité Mixte de Recherche CNRS 2472, Unité Mixte de Recherche INRA 1157 and IFR 115, Bât. 14B, Ave. de la Terrasse, 91198 Gif-sur-Yvette cedex, France. Tel.: 331-69823860; Fax: 331-69824308; E-mail: tavares@vms.cnrs-gif.fr.

Purification of the His₆-tagged Receptor Version YueB780 and Production of Anti-YueB780 Antibodies—Ten-milliliter cultures of strain CG61 carrying pCSJ65 (12) were grown overnight at 28 °C, diluted 100-fold in fresh medium, and incubated in the same conditions until reaching an absorbance at 600 nm of 0.3–0.4. YueB780 production was induced by incubating cultures in a 42 °C water bath for 30 min, and protein synthesis was continued for an additional period of 3 h at 37 °C. Cells were collected by centrifugation (10,000 × *g* for 10 min at 4 °C), resuspended in 20 ml of ice-cold lysis buffer (50 mM Hepes-Na, pH 7.0, 300 mM NaCl, 50 mM imidazole) supplemented with 1 mg/ml fresh lysozyme and a mixture of antiproteases (CompleteTM EDTA-free, Roche Applied Science) and then disrupted by performing three bursts of 1 min (amplitude 60, pulse 3, 30–40 W) in a sonicator (Vibra Cell 72405, Fisher Bioblock, Illkirch, France) with pauses of 1 min. The sample was kept on ice to prevent overheating. Crude extracts were centrifuged (30,000 × *g* for 30 min at 4 °C) to remove insoluble material and the soluble fraction filtered through a pore size of 0.22 μm. The cleared extract was run through a HisTrapTM HP column (Amersham Biosciences AB, Uppsala, Sweden) coupled to an Äkta fast protein liquid chromatography system (Amersham Biosciences AB, Uppsala, Sweden). The column was eluted with a linear gradient of 50–500 mM imidazole in receptor buffer (50 mM Hepes-Na, pH 7.0, 300 mM NaCl). Partially purified YueB780 was then applied to a Superose 6 column (Amersham Biosciences AB) equilibrated in receptor buffer and run at a flow rate of 1 ml/min. Pure YueB780 was kept in receptor buffer at 4 °C for short periods or at –80 °C for long term storage. All receptor concentrations were calculated for YueB780 dimers. SDS-PAGE, Western blot, and protein concentration determination were carried out as described previously (12). Analytical size exclusion chromatography was carried out in a prepacked Superose 6 column (Amersham Biosciences AB) calibrated and run as described previously (16). The Stokes radius derived from the K_{av} value of YueB780 was determined by extrapolation from a plot of Stokes radii of standard proteins versus $(-log K_{av})^{1/2}$ in which $K_{av} = (V_e - V_0)/(V_t - V_0)$, where V_e is the elution volume of the protein, V_0 is the column void volume, and V_t is the column total volume accessible to solvent (16). The standard proteins used were thyroglobulin (Stokes radius = 8.5 nm), ovalbumin (3.05 nm), and myoglobin (2.07 nm). Rabbit polyclonal anti-serum was raised against purified YueB780, and IgG was purified by affinity to protein-A-Sepharose using standard methods (17).

Analytical Ultracentrifugation—Sedimentation velocity measurements were carried out as described previously (18). Data were analyzed to provide the apparent distributions of sedimentation coefficients using the programs Svedberg (19) and DC/DT (20). The solvent density was 1.01081 g/cm³, and YueB780 partial specific volume (0.7219 cm³ g⁻¹) was calculated using the SEDNTERP software (19). Equilibrium sedimentation of YueB780 was performed at 6,500 rpm,⁴ 25 °C. Radial scans at 276 nm were taken at 4-h intervals. Equilibrium was reached after 24 h of centrifugation. The base line was recorded at 60,000 rpm at the end of the experiment. The data were analyzed to yield weight-average molecular weights using the programs XLAEQ and EQASSOC supplied by Beckman Instruments.

Analysis of SPP1-Receptor Interaction, Phage Inactivation, and DNA Ejection—Approximately 5 × 10⁹ SPP1 plaque-forming units (pfu) were mixed in melting ice with different amounts of purified receptor in a final volume of 10 μl. After 30 min on ice, the reaction volume was brought to 40 μl with ejection buffer (100 mM Tris-Cl, pH 7.5, 300 mM NaCl, 10 mM MgCl₂), resulting in mixtures with ~10¹¹ pfu/ml (0.17 nM

and different concentrations of receptor (from ~1 to 17 μg/ml, i.e. ~5.7–97.3 nM YueB780 dimers). The samples were then incubated for 3 h at 37 °C with DNase (10 μg/ml). In an identical experiment, phage SPP1 was mixed with a fixed concentration of receptor (30 nM) and incubated at different temperatures (0, 8, 15, 23, and 37 °C) for 3 h. Half of the mixtures from both experiments was used for phage titration in *B. subtilis* YB886, and the other half was processed as described previously (21) and resolved by agarose gel electrophoresis. Quantification of DNA band intensity was made using the KODAK 1D version 3.5.2 software (Kodak). To determine the rate of SPP1 inactivation (I_r) at different receptor concentrations, ~10¹¹ pfu/ml SPP1 phages were equilibrated at 37 °C in ejection buffer and then the receptor added at the final concentrations of 20, 40, 80, and 200 nM. At different times after receptor addition, aliquots were collected for SPP1 titration. For the calculation of I_r , phage titers were plotted as a function of time and the slopes of the resulting curves determined ($I_r = \ln(P_0/P)/\Delta t$, where P_0 is the initial phage titer and P , the phage titer after a Δt period). The inactivation constant (K_i) was calculated by normalization of I_r according to the input concentration of the receptor ($K_i = I_r \cdot [C]_R^{-1}$). The number of viable phages was determined by titration in parallel to each experiment, and the titer obtained was then used for accurate calculation of phage particle concentration and phage/receptor ratios.

Electron Microscopy—YueB780 was prepared for electron microscopy observation by negative staining with 1% (w/v) uranyl acetate or liophylization by freeze drying followed by heavy metal rotary shadowing with platinum and carbon at an angle of 18° (22). Phages, phage-YueB780 complexes obtained by co-incubation at 4 °C for 1 h, and phages that ejected their DNA after incubation with YueB780 at 37 °C for 2 h were imaged after negative staining (23) or adsorption to mica (24). Immunolabeling with purified anti-YueB780 IgG followed by attachment of protein A complexed to colloidal gold was carried out as described previously (25).

Bioinformatics—Primary sequence homology searches were carried out using PSI-BLAST. SignalP version 3.0 and TMHMM were used for the prediction of signal peptides, transmembrane segments, and membrane topology. Secondary structure predictions were made with PSIPRED. YueB regions potentially involved in coiled coil formation were identified with COILS, and the presence of heptad repeats was detected with PEPWHEEL.

RESULTS

Bioinformatics of YueB—Analysis *in silico* of the YueB primary sequence (1076 amino acids, ~120 kDa) revealed the presence of a putative N-terminal signal peptide and predicted that five transmembrane segments are localized in its C terminus (Fig. 1A). This organization strongly suggested that YueB has a large extracellular domain (ectodomain) of ~800 amino acids. YueB is mostly detected in membrane-enriched fractions of *B. subtilis* cells, confirming that the receptor is associated to the membrane (12). Furthermore, data presented below demonstrated that the receptor ectodomain is exposed to the bacterial surface. Secondary structure predictions suggested that the ectodomain has the propensity to form long α-helices. Three of these putative α-helical regions (amino acids 172–236, 363–408, and 516–611) exhibited also the potential to form coiled coil structures. The segments spanning residues 524–544 and 560–607 include three and seven heptad repeats, respectively, containing the motif abcdefg. Residues a and d, which are localized in the same side of the putative helix, are occupied by hydrophobic residues. Position a is predominantly occupied by isoleucine or leucine, and b is usually leucine (consensus sequence (I/L)X(E/D)LXXX). These heptads confer an amphipathic

⁴ The abbreviations used are: rpm, revolutions/min; pfu, plaque-forming unit(s).

Virus Receptor of a Gram-positive Bacterium

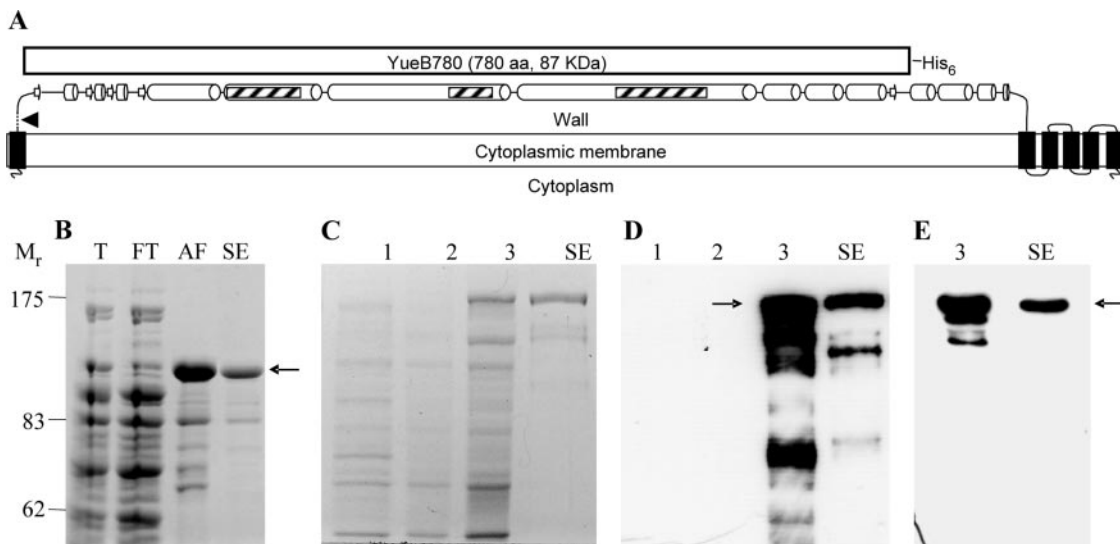


FIGURE 1. Prediction of YueB secondary structure and purification of the ectodomain YueB780. *A*, predicted membrane topology and putative secondary structure of the receptor YueB using TMHMM version 2.0, PSIPRED, and COILS analysis. β -strand and α -helix are depicted as *arrows* and *cylinders*, respectively. Transmembrane and coiled coil segments are represented as *black* and *slashed rectangles*, respectively. The putative cleavage site of the predicted signal peptide sequence is indicated by an *arrowhead*. The region of YueB spanned by the ectodomain YueB780 is depicted at the *top* of the scheme. *B*, SDS-PAGE analysis of the purification of YueB780. YueB780 is indicated by the *arrow*. M_r , molecular weight marker. *T*, total protein extract from an induced culture of *E. coli* strain CG61 carrying pCSJ65. *FT*, flow through of the metal chelate affinity chromatography. *AF*, YueB780 peak eluted from the metal chelate affinity chromatography. *SE*, YueB780 peak obtained from size exclusion chromatography (Superose 6 column). *C–E*, evaluation of YueB780 production and purity by SDS-PAGE and Coomassie Blue staining, Western blot with anti-YueB780, and Western blot with anti-hexahistidine sera, respectively. *Lane 1*, total protein extract from *E. coli* strain CG61 carrying pVEX2.3d (control extract). *Lanes 2 and 3*, total protein extract obtained from non-induced and induced cultures of *E. coli* strain CG61 bearing pCSJ65, respectively. *SE* and *arrows* are as described for *B*.

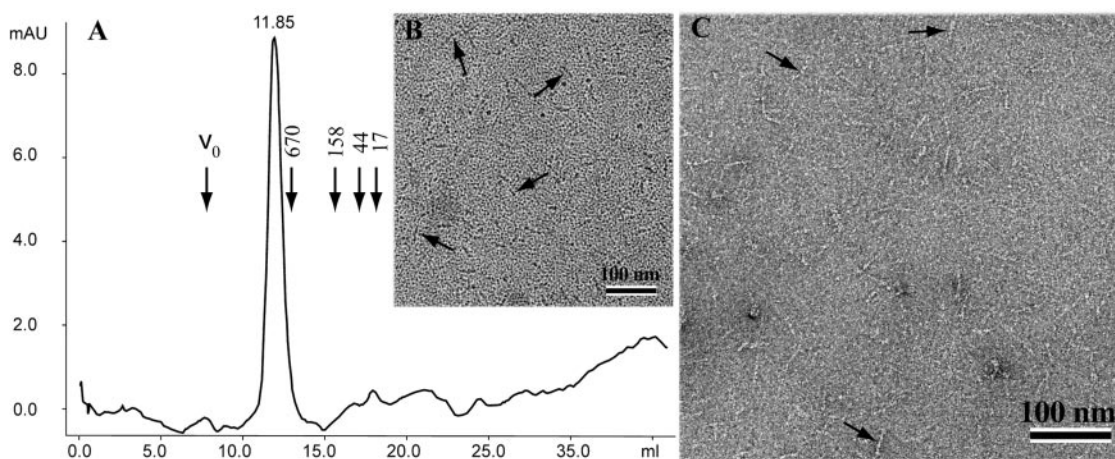


FIGURE 2. Characterization of YueB780. *A*, analytical size exclusion chromatography of YueB780. A 200- μ l sample of YueB780 purified through Superose 6 preparative chromatography was applied to an analytical Superose 6 column. The run was performed with a flow rate of 1 ml/min at 16 °C with continuous monitoring of the eluting material at an absorbance of 280 nm. The column void volume (V_0) determined with blue dextran 2000 (Amersham Biosciences AB) and the volume of elution of standard proteins with the mass shown (bovine thyroglobulin, 670 kDa; bovine gammaglobulin, 158 kDa; chicken ovalbumin, 44 kDa, and horse myoglobin, 17 kDa (Bio-Rad)) are indicated by *vertical arrows*. The *inset* (*B*) shows a micrograph of freeze-dried YueB780 after heavy metal rotary shadowing. *C*, negative staining of purified YueB780. *Arrows* indicate YueB780 fibers. *mAU*, milliabsorbance units.

character to the helices found in coiled coil structures that are involved in the oligomerization of numerous proteins (26). The pattern of long helices in the ectodomain was found on a large number of proteins from Gram-positive bacteria that have sequence similarity to YueB (data not shown) (12). Heptads and coiled coil regions were also identified in a significant number of those protein homologues (not shown).

Purification of the YueB Ectodomain—We overproduced and purified a soluble histidine-tagged polypeptide spanning residues 30–797 of YueB (YueB780) (Fig. 1A) (12). YueB780 was purified from total protein extracts by metal affinity chromatography followed by size exclusion chromatography. The protein had a high tendency to aggregate at NaCl concentrations below 300 mM. In solutions with higher salt concentration, it behaved essentially as a monodisperse species (see “YueB780 Is

an Elongated Dimer in Solution”). During the purification procedure, we were unable to eliminate some minor polypeptides that had a molecular weight lower than the one expected for YueB780 (Fig. 1B). Most of these species were detected by Western blot in crude extracts of cells producing YueB780 using an anti-YueB780 serum. In contrast, they were not detected in control extracts from non-induced cultures of the same bacterial strain, showing that they were truncated versions of the ectodomain rather than contaminant *E. coli* proteins (Fig. 1, C and D). The truncated versions lacked the YueB780 C terminus fused to the hexahistidine tag as revealed by Western blot with anti-hexahistidine serum that detected only the full size protein (Fig. 1E). Co-purification of truncated polypeptides with YueB780 suggested that they associate with the tagged ectodomain. YueB780, with a predicted molecular mass

of 87.3 kDa, had an abnormal migration in SDS-PAGE corresponding to a protein with an apparent molecular mass of ~120 kDa.

YueB780 Forms a Fiber Structure—Native YueB780 eluted as a single peak with an apparent molecular mass slightly larger than 670 kDa from size exclusion chromatography (Fig. 2A). The Stokes radius of the molecule derived from its elution volume is 9.6 nm. The apparent mass and the hydrodynamic radius obtained are incompatible with the expected molecular mass of a globular, monomeric YueB780. Observation of YueB780 freeze-dried and shadowed with platinum-carbon (Fig. 2B) or negatively stained (Fig. 2C) showed that it forms fiber-shaped particles. At high concentrations (0.1 mg/ml), these particles had some heterogeneity in length, probably because of the head-to-tail association of fibers. However, a large majority of the population of molecules observed were particles with identical dimensions when serial dilutions of the protein were imaged in a range of concentrations from 0.1 mg/ml to 0.001 mg/ml. The fibers were 36.5 ± 2.5 nm long and 2.8 ± 0.5 nm thick ($n = 30$) (Fig. 2, B and C, arrows).

YueB780 Is an Elongated Dimer in Solution—To investigate whether the elution behavior of YueB780 from the size exclusion column and the shape in the electron microscope were due to its oligomerization or to its non-globular nature, we carried out analytical ultracentrifugation measurements. Fig. 3A shows sedimentation boundaries of YueB780 at equally spaced times. Raw data (symbols) were modeled to a one- or two-component system. The best fit (solid lines) yielded a single species with a sedimentation coefficient ($s_{20,w}^0$) of 7 S, incompatible with that of a 87.3-kDa globular protein. No rapidly sedimenting material was detected while the rotor was accelerating to reach the operating speed (30,000 rpm), ruling out the presence of large aggregates.

YueB780 was also subjected to sedimentation equilibrium. The average molecular mass of YueB780 in aqueous solution was found to be $164,216 \pm 45$ Da (Fig. 3B), which is very close to the mass expected for a YueB780 dimer (174.6 kDa). The frictional ratio value (f/f_0) calculated for the YueB780 dimer based on its experimental mass and sedimentation coefficient was 1.65. This value deviated significantly from the frictional coefficients of globular proteins ($f/f_0 \sim 1.2$). It strongly suggested that YueB780 is asymmetrical, consistent with the elongated shape of a polypeptide having the dimensions determined from the electron microscopy measurements (axial ratio $a/b = 12.6$). The hydrodynamic radius of YueB780 determined using its experimental molecular mass and sedimentation coefficient is 6.08 nm. The discrepancy between this value and the Stokes radius derived from size exclusion chromatography is likely because of an inaccurate correlation, in the latter method, between the elution volume of very elongated molecules and the Stokes radius (27).

YueB780 Inactivates SPP1 and Triggers Phage DNA Ejection—When YueB780 was incubated with SPP1 virions at 37 °C, the phage titer decreased as a function of the receptor concentration showing that YueB780 bound and inactivated phage SPP1 (Fig. 4A). Considering the linear region of the phage inactivation curve (Fig. 4A), the concentration of YueB780 dimers required to inactivate 99% of the viable phage particles was 28.6 nM. This corresponded to a ratio of ~130 YueB780 dimers/phage particle. Half of the phage/receptor mixtures used in the inactivation experiment was treated with proteinase K to inactivate the DNase present in the samples and to disrupt virions. After deproteinization, the samples were subjected to agarose gel electrophoresis to quantify the DNA remaining inside the phage structures. The amount of protected phage DNA decreased as a function of the YueB780 concentration, reaching a minimum of 0.5–1% of protected DNA relative to the total amount of DNA present in the phages used in the assay (Fig. 4, A and B). SPP1 binding to the receptor fiber thus triggered exit of the

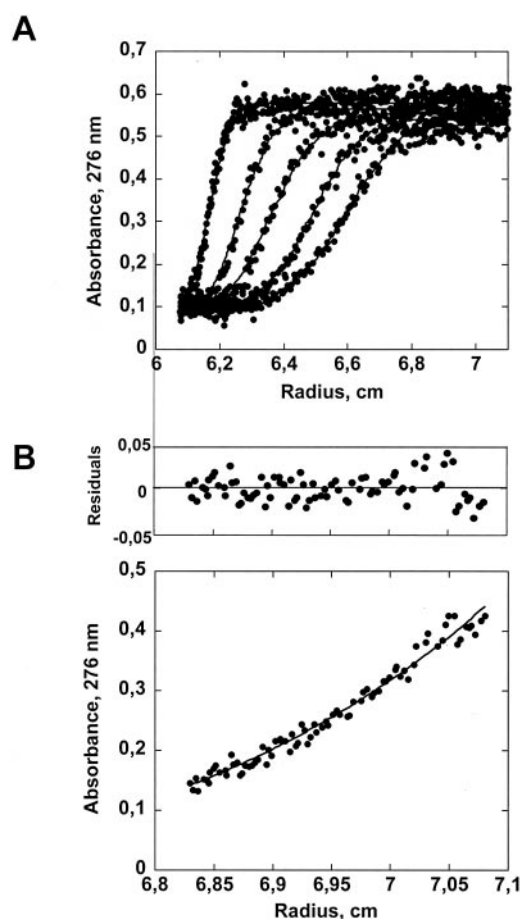


FIGURE 3. Oligomeric state of YueB780. A, sedimentation velocity of YueB780 (1.1 mg/ml in 50 mM Hepes-Na, pH 7.0, 300 mM NaCl). The positions of the moving boundaries shown were recorded at 18-min intervals by spectrophotometric scanning at 276 nm. The solid lines are best fits of the experimental data (●) to a single species model (see "Results"). Rotor speed was 30,000 rpm and temperature, 25 °C. B, measurement of the molecular mass of YueB780 by equilibrium ultracentrifugation. The loading concentration was 1.1 mg/ml of protein. The data (●) obtained at 15 °C and 6,500 rpm for YueB780 were fitted using a dimer model (solid line). The top panel shows the deviation of the data from the fitted curve. The best fit of the data points was obtained for a molecular mass of $164,216 \pm 45$ Da.

phage DNA from the capsid, making it accessible to DNase attack. Note that the inactivation of infective phages was more drastic than the reduction of protected DNA in response to increasing concentrations of YueB780 (Fig. 4A). This was likely due to the presence of particles defective for DNA ejection within the SPP1 population. In such case, the DNase protection assay provided an underestimation of the extent of DNA release from virions competent for DNA ejection. The inactivation rate of SPP1 infectious particles in the presence of YueB780 exhibited a linear dependence on the concentration of the receptor within the range tested (20–200 nM YueB780), yielding an average inactivation constant of $2.93 \times 10^{-3} \pm 0.82 \times 10^{-3} \text{ min}^{-1} \cdot \text{nM}^{-1}$ at 37 °C (Fig. 4C).

Phage genome ejection triggered by YueB780 was temperature-dependent. DNase protection assays showed that no DNA was released at 0 °C. At 8 and 15 °C, a fraction of the phage particles ejected their genome, and frequently the ejection was partial, leading to different sizes of DNA that remained inside the viral capsid, as revealed by the smear of protected DNA (Fig. 4D). This smear was observed at different concentrations of DNase, provided the amount of enzyme was high enough to fully digest free DNA under the experimental conditions used in the assay ($\geq 5 \mu\text{g/ml}$ at 15 °C). Electron microscopy observations further confirmed that a significant number of phages ejected partially

Virus Receptor of a Gram-positive Bacterium

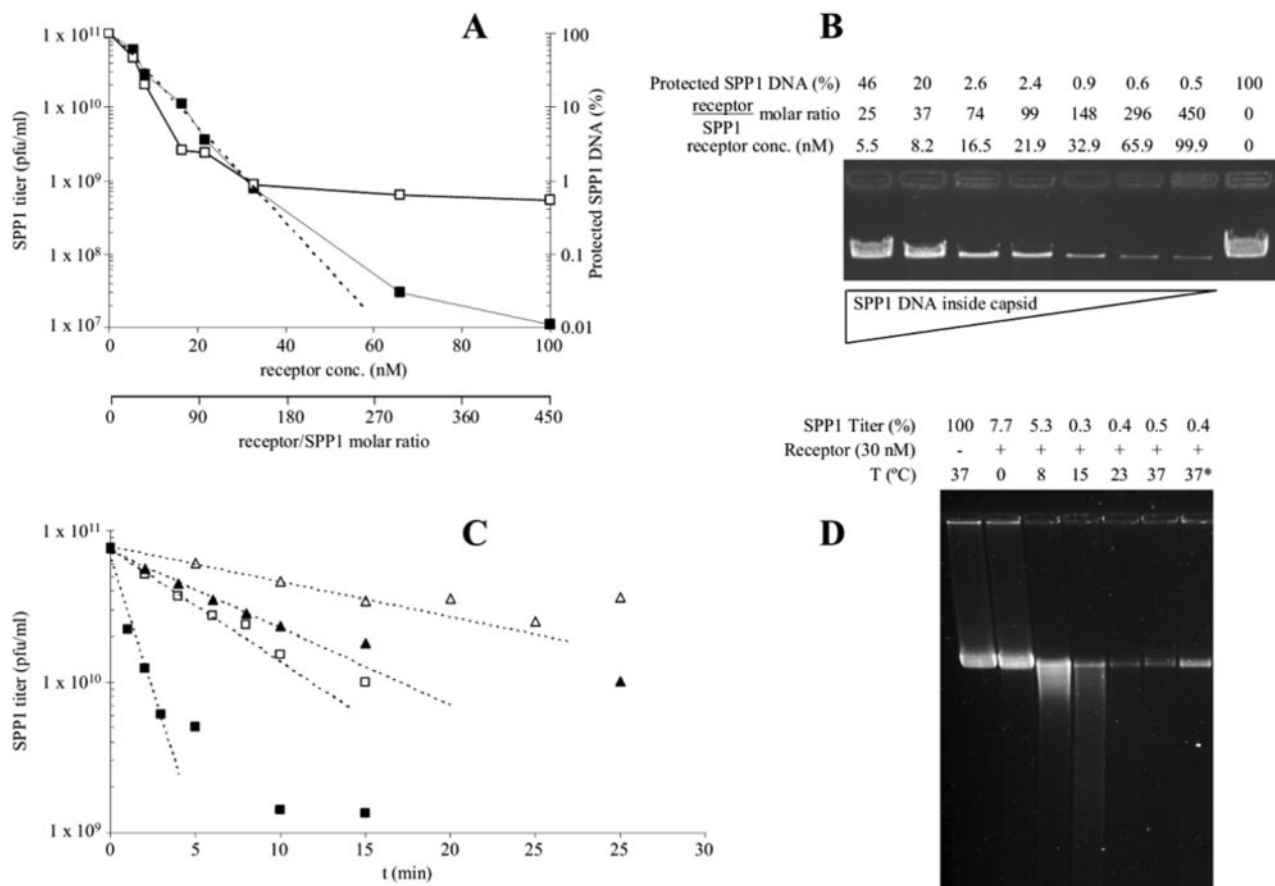


FIGURE 4. Inactivation of SPP1 virions by YueB780. *A*, inactivation of phage SPP1 at 37 °C as a function of receptor dimer concentration (*conc.*) (■). The initial concentration of viable phages in the assay was 1.34×10^{11} pfu/ml (0.22 nM). The *dashed curve* represents the linear correlation between surviving phages and the YueB780 concentration. The amount of DNA remaining protected inside SPP1 virions in the same samples was determined by densitometry of the agarose gel shown in *B* (□) (arbitrary units in the ordinate shown on the *right side*). *B*, triggering of SPP1 DNA ejection by YueB780. Part of the SPP1-YueB780 reactions set up for the inactivation experiment in *A* were deproteinized and analyzed by agarose gel electrophoresis to quantify the amount of DNA remaining protected inside phage structures. *C*, inactivation rate of SPP1 infectious particles (7.66×10^{10} pfu/ml (0.127 nM) were used as initial phage input) in the presence of 20 (△), 40 (▲), 80 (□), and 200 nM (■) receptor dimers at 37 °C. The linear region of the phage inactivation curves (*dashed lines*) was used to calculate the inactivation rate (*I*) of SPP1. *D*, inactivation of phage SPP1 and ejection of its DNA after 3 h incubation with 30 nM receptor, at the temperatures (*T*) indicated. The titer of viable phages is presented as the percentage of the titer obtained in the control sample (no receptor added, 37 °C). The DNase protection assay was as described for *B*. In *lane 37*, DNA ejection was carried out at 37 °C in the absence of DNase. Thereafter, the mixture was equilibrated to 0 °C and the ejected DNA digested with DNase for 3 h at this temperature.

their DNA within the time course of the experiment (not shown). Genome ejection at 23 °C was as efficient as at 37 °C (Fig. 4D). Phage inactivation at different temperatures did not correlate well with the DNase protection assays. At 4 °C, for example, ejection was completely inhibited, but >90% of the phages were still inactivated (Fig. 4D). This discrepancy suggested that serial dilutions of the mixtures in chilled TBT buffer (for phage titration; 100 mM Tris-Cl, pH 7.5, 100 mM NaCl, 10 mM MgCl₂) did not lead to dissociation of the virus-receptor complexes, allowing phage genome ejection after plating.

Visualization of SPP1-YueB780 Complexes—Fig. 5, *A* and *B*, shows electron micrographs of SPP1 virions with their DNA-filled head, tail, and tail spike structures. When SPP1 virus particles were incubated with YueB780 at 4 °C, their tail spike associated with YueB fiber structures (Fig. 5C, *arrow*). This interaction was confirmed using anti-YueB780 IgG that cross-linked SPP1-YueB780 complexes through the phage tail tip region and by labeling of IgG with protein A-gold (Fig. 5D). Despite binding to the receptor, almost all phages presented their heads filled with DNA, even after 72 h at 4 °C (incubation on ice inside a refrigerator). Incubation at 37 °C, with or without a preincubation at 4 °C, led to release of DNA from the vast majority of the virions (Fig. 5, *E* and *F*), as anticipated from biochemical experiments (Fig. 4). Visual inspection of micrographs of the tails before and after DNA ejection did not reveal structural differences (Fig. 5, *A–F*), with the exception of some stain

penetration in the phage tail tube (Fig. 5, *E* and *F*), indicating that it had opened to allow DNA passage to the solution (Fig. 5G). These results showed that SPP1 DNA ejection, but not receptor binding, is a temperature-dependent process.

The YueB Receptor Is Exposed at the Cell Surface—*B. subtilis* cells were incubated with anti-YueB780 antibodies to investigate whether the receptor is exposed to the bacterial surface. The rate of SPP1 irreversible adsorption to these bacteria was significantly lower than that observed with cells treated with an irrelevant antibody (anti-UL25 of HSV-1) or untreated (Fig. 6A). The adsorption constant (K_{ads}) to bacteria pre-incubated with anti-YueB780 ($0.41 \text{ min}^{-1} \cdot U_A^{-1}$) was ~2.5-fold lower than that obtained in the other two conditions ($K_{ads} = 1.11$ and $0.99 \text{ min}^{-1} \cdot U_A^{-1}$, respectively). Therefore, the YueB region displaying SPP1 receptor activity is exposed at the cell surface and is specifically masked by the binding of anti-YueB780 antibodies. Immunogold staining of cells incubated with anti-YueB780 IgG confirmed the localization of YueB780 at the *B. subtilis* surface (Fig. 6B). No labeling was observed in the *yueB* deletion mutant strain CSJ1 (not shown).

DISCUSSION

YueB is a membrane protein of *B. subtilis* that serves as a receptor for the irreversible adsorption of bacteriophage SPP1 (12). We have purified an ectodomain of YueB that bound to the SPP1 tail tip and triggered

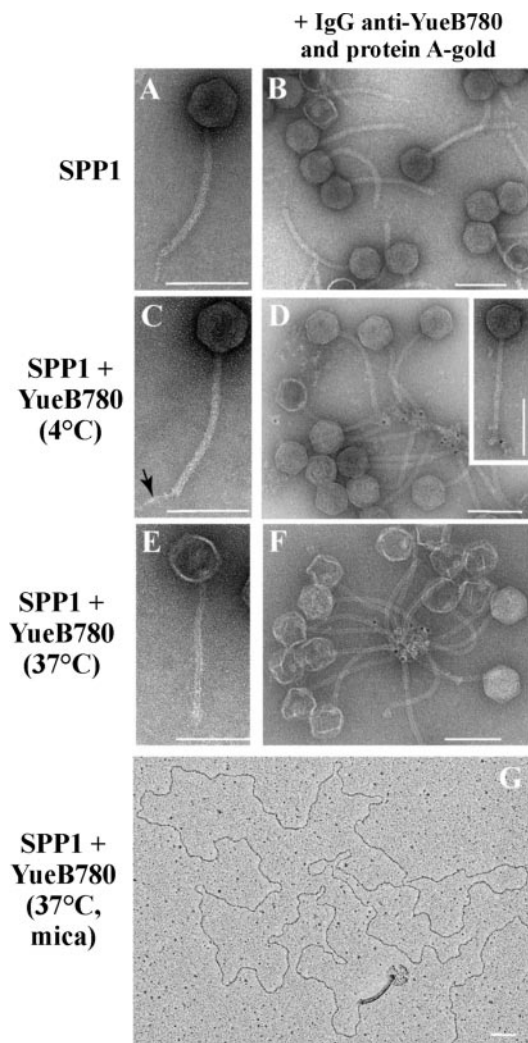


FIGURE 5. SPP1-YueB780 interaction and ejection of phage DNA. SPP1 isolated virions (A and B) incubated with YueB780 at 4 °C (C and D) or at 37 °C (E and F) were negatively stained with uranyl acetate and observed by electron microscopy. The arrow in C shows the position of a YueB780 fiber. The position of YueB780 binding to SPP1 virions was further documented by cross-linking with anti-YueB780 IgG and labeling with protein-A complexed with colloidal gold (D and F). The inset in D shows the position of YueB780 bound to the SPP1 tail tip. SPP1 DNA ejection after incubation with YueB780 at 37 °C is characterized by emptying of the virion capsid structure and some penetration of stain in the tail tube (E and F). The DNA ejected under these conditions was visualized by adsorption to mica (G). The scale bar represents 100 nm.

ejection of viral DNA. YueB780 formed an elongated dimer that behaved like a rod in solution. Its shape explained the abnormal migration in SDS-PAGE and the early elution from size exclusion chromatography columns. The dimer is likely stabilized by a coiled coil between α -helices of the two polypeptide chains. This structure, which stabilizes α -helices through a very efficient burial of hydrophobic side chains (28), is found in many cellular and extracellular structural proteins (streptococcal M proteins, keratins, and tropomyosin (26, 29)) and in virus particles (30–32). The properties of the YueB780 ectodomain are consistent with a dimeric YueB molecule forming an elongated fiber bound to the cytoplasmic membrane via 10 transmembrane segments. Because the putative N terminus signal peptide was not shown experimentally to be cleaved off from YueB, we cannot exclude the possibility that the fiber is fixed to the membrane both at the N and C termini. However, the fiber needs to be long enough to cross the \sim 30-nm-thick peptidoglycan cell wall of the Gram-positive bacterium (33) to expose a receptor domain to the medium (Fig. 6). Considering this requirement and the length of the ectodomain (36.5 nm), the most likely possibility is that YueB is attached to the cell membrane only through its C terminus. The YueB780 rod-like shape probably facilitates the accommodation of the ectodomain within the peptidoglycan mesh. These novel structural features for a virus receptor likely apply to the large family of proteins homologous to YueB that are found in Gram-positive bacteria and that share the same predicted membrane topology and secondary structure (12). Although the physiological function of these proteins remains unclear, their properties make them very suitable receptors for viruses of Gram-positive bacteria.

YueB780 bound to the tail tip of SPP1 and triggered efficiently the release of phage DNA in the absence of other bacterial proteins (Figs. 4 and 5). The inactivation rate of SPP1 virions in the presence of 200 nM YueB780 (0.82 min^{-1}) (Fig. 4C) was identical to the one obtained when phages are added to cultures of *B. subtilis* at a density of $10^8 \text{ cfu}\cdot\text{ml}^{-1}$ (12). The ratio used in the *in vitro* assay was 1500 YueB780 dimers/phage (200 nM receptor for 0.127 nM phage), which, if maintained in the context of SPP1 infection, would imply the presence of 150 active receptors/bacterium (inactivation rates are determined at an input multiplicity of 1 phage/10 bacteria). This number is very probably an overestimation, because during infection, the virus receptors are clustered in large particles (the bacterium), and the very efficient reversible adsorption of SPP1 to *B. subtilis* increases significantly the local concentration of phages at the bacterial surface.

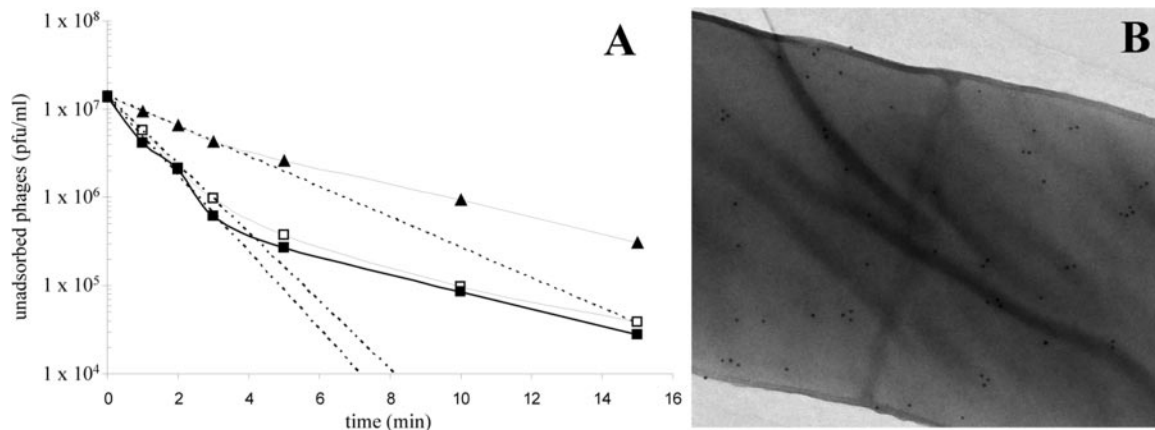


FIGURE 6. Localization of YueB780 at the surface of *B. subtilis* cells. A, kinetics of SPP1 irreversible adsorption to untreated *B. subtilis* cells (■) and pretreated with anti-YueB780 (▲) or anti-UL25 HSV-1 (□) sera. The dashed lines represent the adsorption rates used for K_{ads} determinations. B, labeling of *B. subtilis* CSJ3 (12) with anti-YueB780 antibodies followed by visualization with protein A complexed with colloidal gold (electrodense dots). Bacteria were washed in phosphate-buffered saline and fixed in 1% glutaraldehyde prior to antibody reaction.

Virus Receptor of a Gram-positive Bacterium

YueB780 bound to SPP1 at different temperatures, but DNA release was only efficient above 15 °C. A temperature dependence for DNA ejection was also found for phages λ (34) and T5 (35), showing that there is an energy barrier to triggering DNA release in tailed bacteriophages (36). This barrier is physiologically relevant for phage infection, as it ensures that the virion only ejects its genome to the host cell at temperatures at which that the bacterium is metabolically active. Most interestingly, although SPP1 DNA ejection was fully blocked at 0 °C, partial ejection of the genome occurred in a fraction of the virion population at 8 and 15 °C (Fig. 4D) (electron microscopy observations not shown). Therefore, under these conditions, DNA traffic from the capsid to the phage outside is not a fast all-or-nothing process, because it can be trapped at intermediate stages in the absence of an external counter-pressure to ejection. Our discovery indicates that the molecular event controlling DNA ejection in a temperature-dependent manner affects DNA movement. The DNA end that first exits the phage capsid during ejection is the one that is fixed to a structure-named connector. The connector is found at the tail extremity opposite to the tail tip, forming the tail-capsid interface. SPP1 DNA ejection thus requires that, following receptor binding to the tail tip, a signal is transmitted along the tail helical structure leading to the opening of gp16 (the protein that closes the connector pore) (37), allowing movement of DNA along the tail tube. The conformations of the open connector or of the tail tube at low temperatures are the most conceivable factors in constraining DNA passage. This feature adds to the growing evidence that DNA exit during ejection is not a mere function of the internal pressure inside the capsid (38) but that the phage structure also has active control over the DNA movement process (39, 40).

YueB780 is the first active virus receptor of a Gram-positive bacterium that was purified. Its molecular properties differ radically from the well characterized receptors found in Gram-negative bacteria, which are the outer membrane pore-forming proteins LamB and FhuA (5–7). As anticipated from the properties of Gram-positive bacteria surfaces, the YueB molecule is designed to cross the thick peptidoglycan cell wall, exposing the receptor domain to the extracellular medium. Its fiber structure is unlikely to provide a channel for viral DNA traffic. Because the binding of SPP1 to YueB triggers DNA ejection very efficiently, this raises the question as to how the phage-receptor interaction *in vivo* is coordinated with the efficient routing of viral DNA through the cell wall and membrane to reach the host cytoplasm.

Acknowledgments—We are indebted to Dr. Fatima el Khadali for carrying out analytical ultracentrifugation experiments. We thank Dr. Anabela Isidro for U1L25 anti-serum.

REFERENCES

1. Poranen, M. M., Daugelavicius, R., and Bamford, D. H. (2002) *Annu. Rev. Microbiol.* **56**, 521–538

2. Vinga, I., São-José, C., Tavares, P., and Santos, M. A. (2006) in *Bacteriophage Biology and Biotechnology* (Wegrzyn, G., ed) pp. 165–205, Research SignPost, Kerala, India
3. Hershey, A. D., and Chase, M. (1952) *J. Gen. Physiol.* **36**, 39–56
4. Adams, M. H. (1959) *Bacteriophages*, Interscience Publishers, New York
5. Schirmer, T., Keller, T. A., Wang, Y.-F., and Rosenbusch, J. P. (1995) *Science* **267**, 512–514
6. Ferguson, A. D., Hofmann, E., Coulton, J. W., Diederichs, K., and Welte, W. (1998) *Science* **282**, 2215–2220
7. Locher, K. P., Rees, B., Koebnik, R., Mitschler, A., Moulinier, L., Rosenbusch, J. P., and Moras, D. (1998) *Cell* **95**, 771–778
8. Monteville, M. R., Ardestani, B., and Geller, B. L. (1994) *Appl. Environ. Microbiol.* **60**, 3204–3211
9. Jacobson, E. D., and Landman, O. E. (1977) *J. Virol.* **21**, 1223–1227
10. Davison, S., Couture-Tosi, E., Candela, T., Mock, M., and Fouet, A. (2005) *J. Bacteriol.* **187**, 6742–6749
11. Geller, B. L., Ivey, R. G., Trempey, J. E., and Hettinger-Smith, B. (1993) *J. Bacteriol.* **175**, 5510–5519
12. São-José, C., Baptista, C., and Santos, M. A. (2004) *J. Bacteriol.* **186**, 8337–8346
13. Yasbin, R. E., Fields, P. I., and Andersen, B. J. (1980) *Gene* **12**, 155–159
14. Santos, M. A., de Lencastre, H., and Archer, L. J. (1983) *J. Gen. Microbiol.* **129**, 3499–3504
15. Tabor, S., and Richardson, C. (1985) *Proc. Natl. Acad. Sci. U. S. A.* **82**, 1074–1078
16. Jekow, P., Behlke, J., Tichelaar, W., Lurz, R., Regalla, M., Hinrichs, W., and Tavares, P. (1999) *Eur. J. Biochem.* **264**, 724–735
17. Harlow, E., and Lane, D. (1988) *Antibodies, A Laboratory Manual*, Cold Spring Harbor Laboratory, Cold Spring Harbor, New York
18. Thual, C., Komar, A. A., Bousset, L., Fernandez-Bellot, E., Cullin, C., and Melki, R. (1999) *J. Biol. Chem.* **274**, 13666–13674
19. Philo, J. S. (1994) in *Modern Analytical Ultracentrifugation* (Schuster, T. M., and Laue, T. M., eds) pp. 156–170, Birkhäuser, Boston
20. Stafford, W. F., III (1992) *Anal. Biochem.* **203**, 295–301
21. de Frutos, M., Brasiles, S., Tavares, P., and Raspaud, E. (2005) *Eur. Phys. J. E. Soft Matter* **17**, 429–434
22. Lepault, J., Weiss, H., Homo, J. C., and Leonard, K. (1981) *J. Mol. Biol.* **149**, 275–284
23. Steven, A. C., Trus, B. L., Maizel, J. V., Unser, M., Parry, D. A., Wall, J. S., Hainfeld, J. F., and Studier, F. W. (1988) *J. Mol. Biol.* **200**, 351–365
24. Portmann, R., Sogo, J. M., Koller, T., and Zillig, W. (1974) *FEBS Lett.* **45**, 646–647
25. Lurz, R., Orlova, E., Günther, D., Dube, P., Dröge, A., Weise, F., van Heel, M., and Tavares, P. (2001) *J. Mol. Biol.* **310**, 1027–1037
26. Lupas, A. (1996) *Trends Biochem. Sci.* **21**, 375–382
27. Potschka, M. (1987) *Anal. Biochem.* **162**, 47–64
28. Crick, F. H. C. (1953) *Acta Crystallogr.* **6**, 689–697
29. Phillips, G. N., Jr., Flicker, P. F., Cohen, C., Manjula, B. N., and Fischetti, V. A. (1981) *Proc. Natl. Acad. Sci. U. S. A.* **78**, 4689–4693
30. Carr, C. M., and Kim, P. S. (1993) *Cell* **73**, 823–832
31. Efimov, V. P., Nepluev, I. V., Sobolev, B. N., Zurabishvili, T. G., Schulthess, T., Lustig, A., Engel, J., Haener, M., Aebi, U., Venyaminov, S. Yu., Potekhin, S. A., and Mesyanzhinov, V. V. (1994) *J. Mol. Biol.* **242**, 470–486
32. Andrews, D., Butler, J. S., Al-Bassam, J., Joss, L., Winn-Stapley, D. A., Casjens, S., and Cingolani, G. (2005) *J. Biol. Chem.* **280**, 5929–5933
33. Graham, L. L., and Beveridge, T. J. (1994) *J. Bacteriol.* **176**, 1413–1421
34. Mackay, D. J., and Bode, V. C. (1976) *Virology* **72**, 167–181
35. Tosi, F., Labedan, B., and Legault-Demare (1984) *J. Virol.* **50**, 213–219
36. de Frutos, M., Letellier, L., and Raspaud, E. (2005) *Biophys. J.* **88**, 1364–1370
37. Orlova, E. V., Gowen, B., Dröge, A., Stiege, A., Lurz, R., Weise, F., van Heel, M., and Tavares, P. (2003) *EMBO J.* **22**, 1255–1262
38. Evilevitch, A., Lavelle, L., Knobler, C. M., Raspaud, E., and Gelbart, W. M. (2003) *Proc. Natl. Acad. Sci. U. S. A.* **100**, 9292–9295
39. Manganot, S., Hochrein, M., Radler, J., and Letellier, L. (2005) *Curr. Biol.* **15**, 430–435
40. Kemp, P., Gupta, M., and Molineux, I. J. (2004) *Mol. Microbiol.* **53**, 1251–1265

The Ectodomain of the Viral Receptor YueB Forms a Fiber That Triggers Ejection of Bacteriophage SPP1 DNA

Carlos São-José, Sophie Lhuillier, Rudi Lurz, Ronald Melki, Jean Lepault, Mário Almeida Santos and Paulo Tavares

J. Biol. Chem. 2006, 281:11464-11470.

doi: 10.1074/jbc.M513625200 originally published online February 14, 2006

Access the most updated version of this article at doi: [10.1074/jbc.M513625200](https://doi.org/10.1074/jbc.M513625200)

Alerts:

- [When this article is cited](#)
- [When a correction for this article is posted](#)

[Click here](#) to choose from all of JBC's e-mail alerts

This article cites 36 references, 14 of which can be accessed free at <http://www.jbc.org/content/281/17/11464.full.html#ref-list-1>